PHYSICAL REVIEW B VOLUME 18, NUMBER 4 15 AUGUST 1978

Studies of the Si(111) surface with various Al overlayers

H. I. Zhang* and M. Schlüter
Bell Laboratories, Murray Hill, New Jersey 07974
(Received 27 March 1978)

The electronic structure of the Si(111) surface with Al overlayers has been investigated by the self-consistent pseudopotential method for three different Al chemisorption sites. The geometries are a onefold coordinated covalent site, and two other geometries which correspond to threefold coordinated ionic sites with different Al-Si bond lengths. The electronic energy bands, local densities of states, and charge distributions for some surface states are presented in detail. The results together with those of a previous calculation based on the Lander substitutional geometry are compared to recent photoemission and electron-energy-loss experiments on Si(111) with adsorbed Al overlayers of variable thickness. The study yields structural information on the formation of covalent metal-semiconductor bonds which stabilize the Fermi level and which are believed to be essential in the formation of Schottky barriers.

I. INTRODUCTION

Although much attention has been paid to the understanding of metal-semiconductor interface properties, mainly stimulated by the technological importance of Schottky-barrier (SB) devices,[1] the fundamental theory of the metal-semiconductor interface is still in a rather primitive stage. In particular, the chemical trends of SB properties have not been explained satisfactorily so far. It has been reported experimentally that the SB height ΔV, as measured by C-V or I-V characteristics is quasi-independent of the metal work function or electronegativity, if covalent semiconductors are used. On the other hand ΔV shows strong dependence on the metal properties, if ionic semiconductors are involved. It has been proposed originally[2] that this behavior is a result of a fundamental *covalent-ionic transition* as it also appears, e.g., for structural problems.[3] Subsequently, numerous theoretical studies[4-9] have focused on this behavior without being able to fully explain the fundamental transition. Recently the transition *per se* has been questioned in its existence and more critical data analysis has been proposed.[6,10]

Originally, the concept of Fermi-surface pinning by *surface states*, which in turn determines the SB height, was introduced by Bardeen as early as 1947.[11] The basic ideas of this concept survived until today, in particular, as an explanation of the independence of ΔV for covalent semiconductors such as Si, Ge, and GaAs. At a later stage, Heine[12] modified Bardeen's ideas by replacing the intrinsic surface states by resonances coupled to tails of metal wave functions decaying into the semiconductor. These ideas have recently been put onto quantitative grounds by the work of Louie, Chelikowsky, and Cohen.[7] In their approach a metal-semiconductor interface is represented by a periodic jellium-semiconductor sandwich system. By choosing jellium to represent the metal, they escape the difficulty of atomic arrangement and lattice matching in the interface. Nevertheless, calculating the electronic structure of the system using a self-consistent pseudopotential technique, identical to that used in the present work, they basically confirmed Heine's idea of extrinsic metal-induced states being responsible for the Fermi-level pinning. On the other hand, it has been pointed out by Phillips,[5] that a correct description of the interface properties should involve consideration of chemical bonds in the interface which leads back to the problem of atomic arrangements. To circumvent this problem, Phillips suggested the use of the dielectric theory which has been applied very successfully to bulk semiconductors.[3] A different approach involving dielectric screening has been proposed by Inkson[4] on the basis of a many-body approach. The problem of lattice mismatch in the interface region has been picked up by Varma and Pandey[9] who propose that geometrical disorder in the interface introduces localized many-electron states (as in amorphous glasses) which should stabilize the Fermi level.

In drawing conclusions from the existing theories it appears that a common point of controversy is the existence and nature of localized electronic states in the region of the metal-semiconductor contact. It is obvious that direct experimental input, beyond the integrated electrical SB measurement,[2] is needed to settle this controversy.

Relevant surface-sensitive experimental techniques, capable of yielding details of the local density of states (LDOS) in the interface region have recently been developed and applied to the study of the *formation* of SB on semiconductors as[13-17,21] Si and Ge (Refs. 13 and 15) III-V compounds[13,15,18,19] and II-VI compounds.[20] In these studies the usual bulklike metal-semiconductor devices are replaced by clean semiconductor surfaces with

chemisorbed metallic overlayers of controlled thickness starting as low as submonolayer coverage. This approach offers the interesting theoretical possibility to study, e.g., monolayer chemisorption systems for which the problem of atomic geometrical arrangements seems to be at least tractable. In support, ultraviolet photoemission spectroscopy (UPS)[16] and electron-energy-loss spectroscopy (EELS)[13] results seem to suggest that Fermi-level stabilization occurs almost completely after monolayer coverage and that the behavior of the interface is dominated by the first metal overlayer.

It has been pointed out,[16] however, that caution has to be used in generalizing the detailed experimental microscopic results obtained on a particular metal-semiconductor system to all Schottky barriers. While these experiments suggest that a sufficiently precise and at the same time general theoretical description becomes more and more difficult, they also offer valuable details for studying a particular case, fully accounting for the microscopic details of the chemical bonding in the interface. First examples of studies of this kind have recently been published.[22,23]

In the present paper we present self-consistent pseudopotential calculations of Si(111) surfaces with monolayers of chemisorbed Al. Choosing this system we make direct contact with the measurements of Margaritondo, Rowe, and Christman.[13,17] Including the recent work of Chelikowsky,[23] who studied the Si(111)-Al system in the so-called Lander substitutional geometry,[24] the present studies provide a complete microscopic theoretical analysis of this particular metal-semiconductor interface system.

We shall continue in Sec. II by reviewing the employed methods of calculation. Section III will be devoted to a description of the theoretical results, which in Sec. IV will be compared to experiments. The main results of this study are summarized in Sec. V.

II. METHODS OF CALCULATION

The present calculations are performed by the self-consistent pseudopotential method based on a slab geometry which retains artifical periodicity perpendicular to the surface.[25]

The slabs extend parallel to the Si(111) surface and consist of 12 Si atomic layers and one Al overlayer on each side. The slabs are periodically repeated allowing a separation of about three to four Si-Si bond lengths between each other. Three different geometries have been assumed for the positions of Al atoms chemisorbed on the Si surfaces. The geometries assumed here are similar to those considered by Schlüter *et al.*[26] for the chlorine chemisorption sites in Si(111)-Cl and Ge(111)-Cl. The first geometry (case I) we consider is the onefold coordinated covalent site geometry, in which the Al atoms are located directly on top of Si atoms in the outmost Si layer. The Si-Al bond length here is assumed to be identical to the Si-Si bond length[23] which is taken to be 2.34 Å. The other two geometries are threefold-coordinated ionic-sites geometries in which the Al atoms are located above the center between three atoms of the outermost Si layer and on top of the fourth layer Si atoms. Bond-length determination on the basis of chemical grounds is complicated for these quasi-ionic configurations. Thus two cases of different bond lengths are considered as has been done in the Si(111)-Cl studies.[26] In the second geometry (case II), the distance between Al atoms to the nearest Si atoms is assumed to be identical to the Si-Si bond length, and in the third geometry (case III) it is increased by 25%.

In discussing the results we shall also present recent calculations of Chelikowsky[23] carried out in an identical scheme to that used here, but based on Lander's[24] substitutional geometry. In this geometry the outermost Si layer is replaced by Al atoms. Bond lengths have been kept at the bulk Si value of 2.34 Å in the work of Ref. 23. It should be noted that this choice of an Al-Si covalent bond length is justified on chemical grounds, using covalent atomic radii, corrected for ionicity differences.[23] Similar chemical arguments have successfully been used in studying the Si(111)-Cl chemisorption systems.[26]

The second important input quantity into our calculations is the one-electron potential. As described in detail in Ref. 25, ionic pseudopotentials for Al^{3+} and Si^{4+} are needed for the calculations and have to be constructed. At a large distance from the origin these pseudopotentials, of course, behave as $-3e^2/r$ and $-4e^2/r$, respectively. As one approaches the core region, the potentials are smoothly cut off not to yield any core states. The requirements are as follows: First, the ionic potentials reproduce spectroscopic term values over a reasonable energy range for the Al^{2+} and Si^{3+} hydrogenlike systems. Secondly, the potentials, if self-consistently screened by the valence electrons within the Hartree-Fock-Slater (HFS) framework should compare with other self-consistent field calculations which do not employ pseudopotentials.[27] Finally as a third requirement, the potentials should yield accurate Si and Al bulk band structures calculated within the same HFS self-consistent field approach. For the present case the results agree with experimental data to within 0.2 eV which represents the actual state of the art. Since these potentials yield accurate re-

TABLE I. Parameters for ionic pseudopotentials of Eq. (1) and the empirical pseudopotentials of Eq. (3). If q is entered in atomic units the resulting potentials are in Ry. The potentials are normalized to an average atomic volume of Ω_{av} = 158.65 a.u.

V_{ion}	Si	Al
a_1	-0.977 90	-3.650 40
a_2	0.790 65	0.376 00
a_3	-0.352 01	-0.870 00
a_4	-0.018 07	-0.082 40
V_{emp}	Si	Al
b_1	2.414 9	0.433 2
b_2	2.129 0	1.880 0
b_3	0.691 0	0.650 0
b_4	-2.600 0	-0.300 0

sults for the electronic structure of free ions, atoms, and bulk crystals, they should by continuity give accurate results for the surface systems. It should be emphasized that this procedure of determining ionic pseudopotentials, while not being of a first-principles character, still does not contain any parametrization in connection with the surface system. Thus the surface charge distribution will truly be determined self-consistently as a response to ionic Al^{3+} and Si^{4+} pseudopotentials.

The self-consistent pseudopotential employed in our calculation consists of two parts: the ionic pseudopotentials for Si^{4+} and Al^{3+} generated as described above and the HFS screening potential due to the valence electrons. The ionic pseudopotentials are for convenience expressed in reciprocal space in the form

$$V_{ion}(q) = (a_1/q^2)[\cos(a_2 q) + a_3]\exp(a_4 q^4). \quad (1)$$

The values of parameters a_i are given in Table I. The validity of this expression is tested for the calculation of bulk band structures and numerous surface calculations.[25]

The HFS screening potential due to the valence electrons is determined self-consistently. The Fourier coefficients of this potential corresponding to the reciprocal-lattice $\vec{G}$ can be expressed as

$$V_{HX}(\vec{G}) = 4\pi(e^2/G^2)\rho(\vec{G}) - \alpha(3/2\pi)(3\pi^2)^{1/3}e^2\rho_{1/3}(\vec{G}), \quad (2)$$

where $\rho(\vec{G}), \rho_{1/3}(\vec{G})$ are the Fourier coefficients of the total valence charge density $\rho(\vec{r})$ and the cube root of that density $[\rho(\vec{r})]^{1/3}$, respectively. In the present calculation, the value of α in the exchange potential is taken to be 0.79, as usual.[25] To calculate the Fourier coefficients of the cube root of the charge density the following scheme, proposed by Ho[28] is employed: the charge Fourier coefficients $\rho(\vec{G})$ are transformed into real space values $\rho(\vec{r})$ using "fast Fourier transform" (FFT) programs. The cube root is taken at each point $\vec{r}$ and the inverse FFT routine is employed.

To initiate the self-consitent loop, we start with the empirical atomic pseudopotential, expressed in reciprocal space in the form

$$V_{emp}(q) = b_1(q^2 - b_2)/\exp[b_3(q^2 - b_4)] + 1. \quad (3)$$

The coefficients b_i are given in Table I.

The wave function basis set is represented by approximately 430 plane waves and reduced by Löwdin's perturbation technique to about 160 plane waves. The values correspond to the degree of convergence used in earlier surface work.[25] To evaluate the valence electron charge distribution of each iteration step, the Hamiltonian has been diagonalized for a particularly chosen set of special $\vec{k}$ points.[29] Initially we use one special $\vec{k}$ point, and after obtaining nearly self-consistent pseudopotentials, we refine the self-consistency using a set of three special $\vec{k}$ points. The self-consistent pseudopotential obtained by one special $\vec{k}$ point is shown to be an already reasonably good approximation, and the refined pseudopotential using the three special $\vec{k}$-point set is expected to have even in metallic situations a sufficient degree of accuracy. The iteration steps within the self-consistency loop are treated as in Ref. 23 using a combination the modified Pratt scheme[27] and the attenuated feedback scheme.[25] Self-consistency is generally achieved to the degree that the root-mean-square deviation between the input and output potentials averaged over the slabs be less than 0.3 eV. The energy eigenvalues in this case are stabilized to within 0.1 eV. Once the self-consistency has been obtained, the energy bands and wave functions were evaluated at 28 $\vec{k}$ points throughout the irreducible part of the surface Brillouin zone. To determine the local density of state (LDOS) and the Fermi level, we employed the Gilat-Raubenheimer $\vec{k}$ space integrations method.[30] The analytical representation of the energy bands at each of the 28 $\vec{k}$ points is obtained using a $\vec{k}\cdot\vec{p}$ gradient expansion. The LDOS is expressed as

$$N_L(E) = \sum_{k_{\parallel},n} P_{k_{\parallel},n}(L)\,\delta(E - E_n(k_{\parallel})), \quad (4)$$

where

$$P_{k_{\parallel},n}(L) = \int_L |\psi_{k_{\parallel},n}(r)|^2 d^3r. \quad (5)$$

$\psi_{k_{\parallel},n}$ is the wave function of the nth band at $\vec{k}_{\parallel}$, and L represents the local region of interest. We

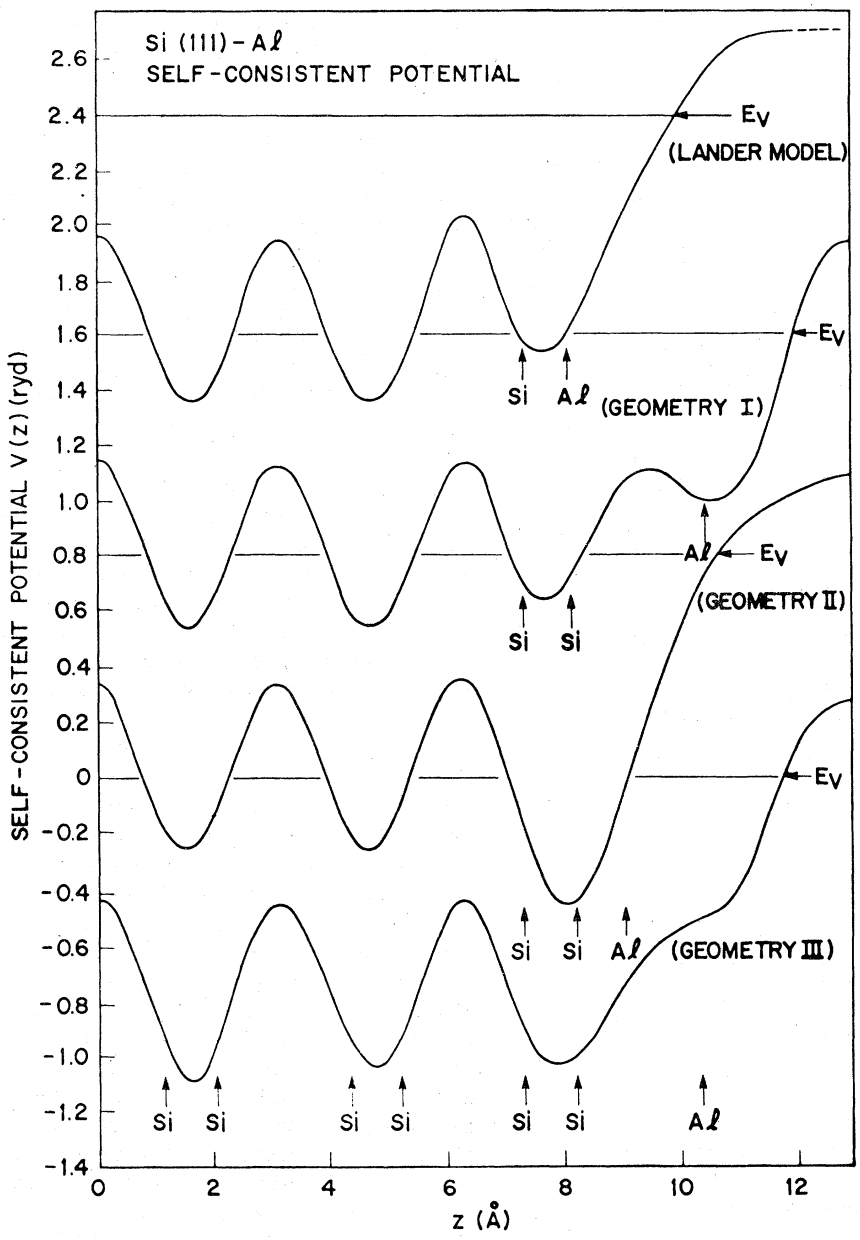

FIG. 1. Self-consistent potentials for three different geometries I, II, and III studied in this paper. Added is the potential for the Lander substitutional geometry which is used in Ref. 23. The atomic positions of the outermost layers are indicated. The potentials are averaged parallel to the surface and the values are given in rydbergs.

divide the slab into local regions parallel to the surface, each of which includes one layer of Si (or Al) atoms. The LDOS spectra are used to identify surface states or resonances. This identification is done in connection with inspecting the real space charge distributions via contour plots of individual states.

III. RESULTS

In this section we report the theoretical results for the potentials, energy bands, local densities of states, and charge densities for the three different geometries (I-III) of the Si(111)-Al system.

In Fig. 1 self-consistent potentials are shown as a function of the coordinate z perpendicular to the surface. The potentials are averaged parallel to the (111) surface. The potentials follow the periodic structure deep inside the bulk as indicated by the atomic positions and then decay into the vacuum with various shapes depending on the overlayer geometry. In addition to the three geometries (cases I to III) studied here, Chelikowsky's results[23] for the Lander model are also shown. The position of the Fermi level is shown for each potential. If one takes the value of the potential in the center of the vacuum region as zero reference, work-function values can be deduced. These values are

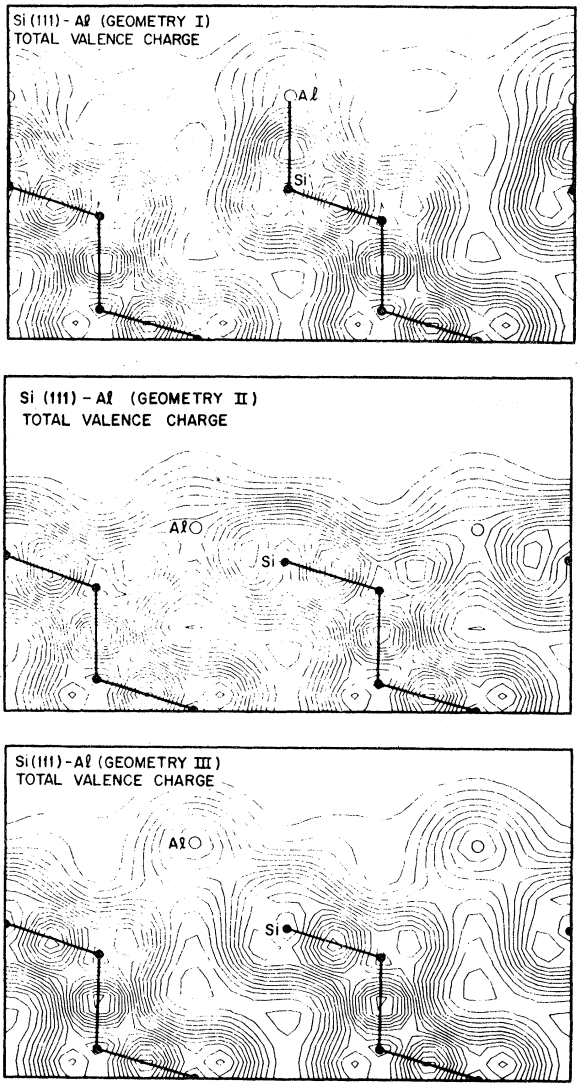

FIG. 2. Contour plots of the total valence charge distributions for the three chemisorption geometries studied in this paper. The contours are plotted in a (110) plane intersecting the (111) surface at right angle. The contours are arbitrarily normalized.

consistently too small as compared to experiment, which obviously is a result of an incomplete decay of the potential as one reaches the center of the vacuum region. As already mentioned in Ref. 23, however, correct trends in changes of the work function are observed as one goes from the clean surface to the metal overlayer surface. The calculated value decreases from about $\phi \approx 4.0$ eV to $\phi \approx 3.5$ eV. Variations depending on the individual overlayer geometry are found to be within the numerical noise of our work-function calculations.

In Fig. 2 contour plots for total valuence charge distributions are shown for the three geometries. The contours are displayed in a (110) plane intersecting the (111) surface at right angles. The charge is plotted over a distance of two surface unit cells parallel to the surface and over five atomic layers perpendicular to the surface. The positions of the Si bulk atoms and Al overlayer atoms are marked by full and open circles, respectively. The charge contours are arbitrarily normalized but comparison with earlier[25] calculations shows identical results for the bulk regions. Very marked differences occur for the three geometries. As expected, only for case I, the "covalent" geometry, a pronounced covalent bonding charge appears. The maximum charge contour in this Si-Al bond is about 10%–15% smaller than for the bulk-like Si-Si bonds which agrees with the results for the Lander model[23] where Al is also covalently bound to Si. For cases II and III, the "ionic" geometries, no clearly identifiable covalent bonding charge shows up, though for case II, with the Al atoms close to the surface, the adjacent Si-Si backbonds are polarized and deformed such that charge is pulled into the Si-Al bonding region. As shall be seen from comparing spectal features with experiment, case II is probably somewhat unrealistic, thus the charge arrangement for an "ionic" geometry should be rather close to the results for case III.

The energy bands along the two major symmetry axes in the hexagonal surface Brillouin zone are presented in Fig. 3 for the three geometries considered here. In this figure, the Si bulk band structure, which has been calculated with the same ionic pseudopotential as used for the surface case, is also indicated. This is, of course, identical to the usual three-dimensional band structure projected onto the two-dimensional surface Brillouin zone (shaded areas). Major surface states and resonances are indicated by dashed lines. Their predominant atomic wave-function character is also indicated. The surface states band structures in the region of fundamental gap are rather different for the three cases. We notice that the occupied surface bands are relatively low in energy in geometry I, thus yielding a lower Fermi level as compared to the other two geometries. For geometry III, the Fermi level does not pass through any surface bands, but is centered in a very small fundamental gap, while the Fermi level passes through surface bands creating electron and hole packets for the other two geometries. Although geometries II and III differ only by a 25% bond-length change, the resulting surface band structures are quite different. One major feature of geometry II is the existence of a split-off Si s band below the bulk band structure. This is in response to the relative short distance of a complete Al overlayer from the Si substrate. In fact, if this layer is

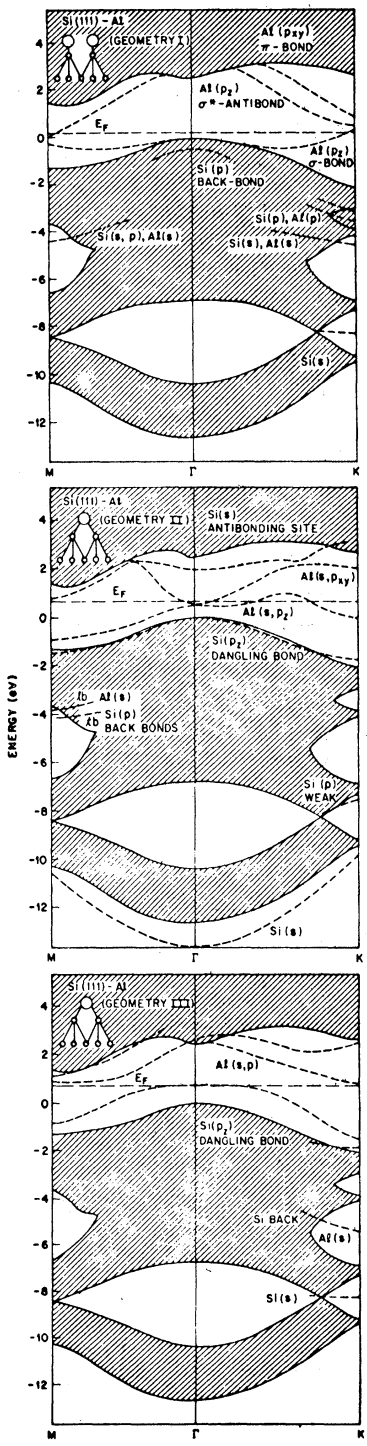

FIG. 3. Two-dimensional $E(k_{\parallel})$ band structures for three geometries of the Si(111)-Al system. The energies are plotted along high-symmetry lines in the two-dimensional hexagonal Brillouin zone. Bulk band regions are indicated by shaded areas, various surface states and resonances are shown by dashed lines and their most prominent characters are indicated. The positions of the Fermi levels are also indicated.

moved outwards as in geometry III the split-off band disappears.

Within and in the immediate neighborhood of the fundamental gap, the surface states for geometries II and III derive mainly from an occupied Si dangling bond and from Al p orbitals. The details of the band structures vary considerably. In particular the Si dangling-bond band is pushed back into the gap region in geometry III, as the Al layer is moved away from the substrate. This is in accord with calculations for the ideal clean Si(111) surface[25] where it is found about midgap, and is half occupied.

The local densities of states (LDOS) for the three geometries are presented in Figs. 4–6. To indicate the chosen local areas the total valence charge profiles are displayed for reference as a function of z perpendicular to the surface. These charge densities are averaged parallel to the surface and should be compared to the potentials in Fig. 1. In general, the LDOS is given for six layers, with the exception of geometry I, for which seven layers are displayed. In addition to comparison with geometries II and III, a combined LDOS for the outermost Si-Al double layer is shown as

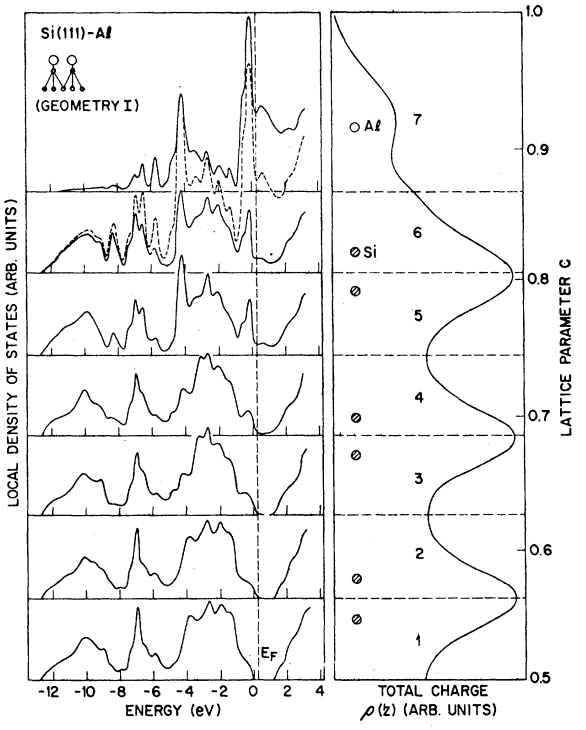

FIG. 4. Local density of states spectrum for geometry I of the Si(111)-Al system. The slab is divided into atomic layers as indicated by the dashed lines in the total valence charge profile which is shown for reference. The dashed curve represents layers six and seven combined.

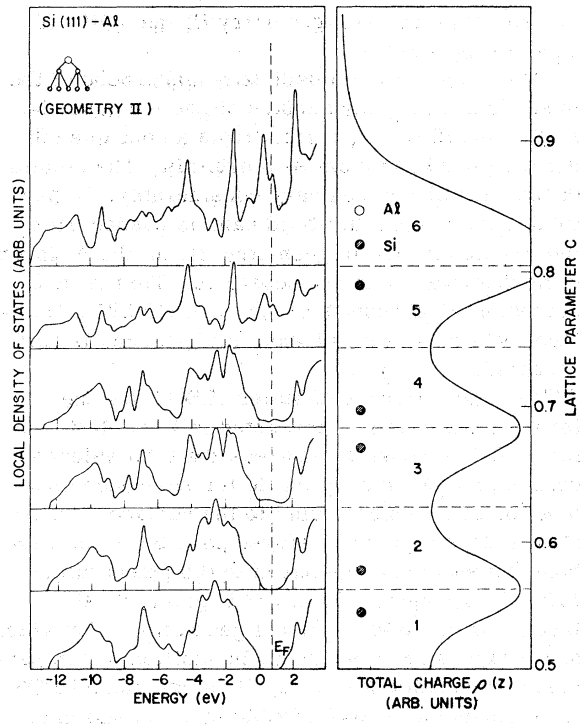

FIG. 5. Local density of states spectrum for geometry II of the Si(111)-Al system. See caption of Fig. 4 for details.

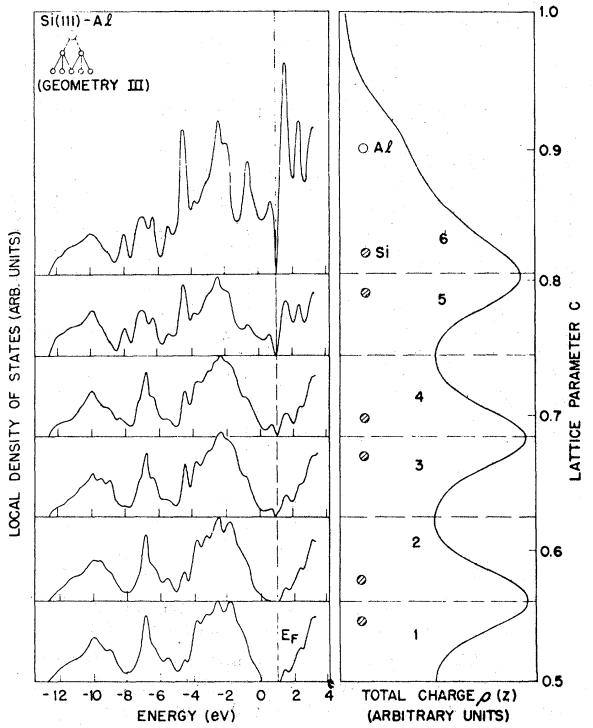

FIG. 6. Local density of states for geometry III of the Si(111)-Al system. See caption of Fig. 4 for details.

dashed line for geometry I. The LDOS for layer 1, deep inside the bulk region are nearly identical for the three geometries and represent a reasonable approximation to the Si bulk density of states. As one approaches the surface several surface features appear. In particular states grow into the Si gap, as already seen on the band-structure plots in Fig. 3, and thus determine the position of the Fermi level.

The Fermi level is found about 0.4 eV above E_v, the top of the valence bands, for geometry I, 0.8 eV for geometry II, and 0.9 eV for geometry III. For the clean surface the Fermi level has theoretically been found around 0.7 eV for the unreconstructed surface and around 0.3 eV for the 2×1 reconstructed surface.[25] We thus find a downwards shift of the Fermi level for geometry I and small upwards shifts for geometries II and III as compared to the clean, unreconstructed surface. The difference in these results may be explained as follows: in geometry I, Al atoms partially saturate the Si dangling bonds, whose energy consequently moves somewhat downwards. The position of the Fermi level is then basically given by the upper edge of this Si-Al bonding band. In geometries II and III on the other hand, the less electronegative Al atoms, which now sit in the "ionic" positions yield charge to the Si surface atoms, i.e., fill their dangling bonds. The exact position of the Fermi level is given by the amount of charge transfer. In general terms, however, for chemisorption of atoms which are less electronegative than the substrate one would expect the Fermi level to move upwards, provided the surface is metallic. This has also been found theoretically for the Lander substitutional geometry[23] where $E_F - E_V \approx 0.9$ eV.

The LDOS spectra of the outermost surface Si-Al double layer for the three geometries studied here and for the Lander model[23] are compared to each other and to the Si bulk spectrum in Fig. 7. Prominent features in the spectra are labeled and listed in Tables II and III together with their energy, $\vec{k}$-space location and associated atomic character. There are two main features at high binding energies resulting mostly from Si s-like surface states, rather similarly for all geometries. An exception is the popping out of an s-like band for geometry II which has already been described in connection with the surface band structure. An individual charge density of these states is shown in Fig. 8.

Peak C between -4.0 eV and -4.6 eV appears surprisingly unaffected by changes in the chemisorption geometry. Its wave-function character is predominantly Al s-like with some Si p admixture. These results are illustrated by Figs. 9 and 10 where the charges of peak C are plotted for

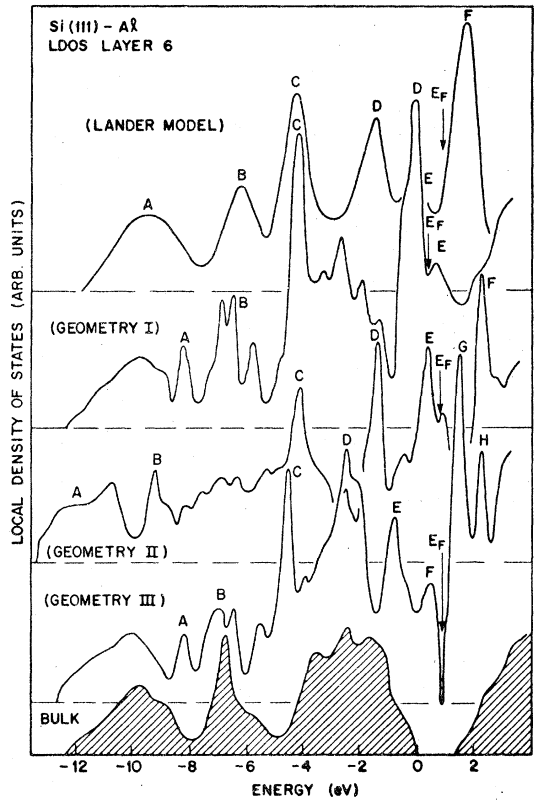

FIG. 7. Comparison of local density of states spectra for the outermost double layer of the different Si(111)-Al models. Four different geometries I, II and geometry III as well as the Lander substitutional geometry used in Ref. 23 are considered. Also shown for comparison is the bulk density of states of Si. The positions of the Fermi level are marked for all geometries.

TABLE II. List of main spectroscopic features in the surface LDOS spectra of all considered chemisorption geometries. The table refers to Fig. 7. All energies are taken with respect to the valence band maximum of Si.

	Energy and k-space location for geometry			
Peak	I	II	III	Lander model
A	-8.2 *K*	<-12.0 all BZ	-8.2 *K*	-8.7 *K*
B	-6.5 *K*	-9.2	-.65 *K*	-6.3 *K*
C	-4.3 *K, M*	-4.1 *K, M*	-4.6 *K*	-4.6 *K, M*
D	0.0 all BZ	-1.7 *K, M*	-2.5 volume	-1.6 *K*
E	0.7 *K*	0.2 Γ-*K*	-1.3 *K*	0.1 *M*
F	...	2.0 *K*	0.7 volume	1.5 all BZ
G	...	...	1.5 *K*	...
H	...	...	2.2 Γ-*K*	...

geometry I (Fig. 9) and geometry II (Fig. 10). Similar results are found in Ref. 23 for the Lander substitutional geometry.

Among the features *D*, *E* (and *F* for geometry III) with lower binding energies, Si and Al *p*-like states are most predominant. The particular atomic characters can be found in Table III and are illustrated by the following charge contour plots. In geometry I peak *D* (Fig. 11) at about 0.0 eV can be regarded as the *p*-like partner of peak *C* (Fig. 9). The two states combined may be regarded as forming the Si-Al σ bond. Peak *D* in geometry II (Fig. 12) around −1.7 eV arises from the original Si dangling bonds which dropped in energy and consequently captured about one electron. Peak *D* in geometry III is at higher binding energy (−2.5 eV) and corresponds to some rather dilute Al *s* and *p* character mixed with Si bulklike states. Peaks *E* in geometry II and *E*, *F* in geometry III again correspond to Si p_z-like states but now with some additional charge pile up on the Al atoms which are placed in the ionic sites (see Fig. 13 for geometry III). The unoccupied conduction states (peaks *F* and *G*, *H* for geometry III) correspond mainly to Al *p*-like orbitals and result from various critical points within the Brillouin zone.

To summarize these rather complicated results we may stress the following simple facts: (a) Below −6 eV only Si associated *s*- and *p*-like surface exist. This is in agreement with the results of the Si(111)-jellium calculations of Ref. 7. (b) The strong feature around −4.5 eV is associated mainly with Al *s*-like states and appears invariably for all geometries. (c) Peaks within 4 eV of the Fermi level appear strongly for all geometries and are either due to unsaturated (dangling-bond-like) Si surface states or to Si-Al bonding states involving *p*-like orbitals. The position of these structures varies with overlayer geometry. No strong features have been found in this region for the Si-jellium case.[7] (d) In all cases Fermi-level pinning occurs due to metal-induced surface bands. (e) The lowest conduction band states are of Al *p*-like character and lead to strong peaks in the surface LDOS for the ionic geometries (cases II and III) and the Lander geometry, but not for covalent geometry (case I). This latter fact is of help to discriminate between possible geometries in nature using electron energy loss spectroscopy.

TABLE III. List of the wave-function character of the main spectroscopic features in the surface LDOS spectra. The table continues Table II.

	Character for geometry			
Peak	I	II	III	Lander model
A	Si *s*-like + backbond	Si *s*-like	Si *s*-like + backbond	Si *s*-like 2nd layer
B	Si *s-p* long. backbond	Si *s*-like	Si *s-p* long. backbond	Si *s*-like 2nd and 3rd layer
C	Al *s*-like Si p_z-like	Al *s*-like Si *p*-like backbond	Al *s*-like Si *p*-like backbond	Al *s*-like
D	Al p_z-like σ bond	Si p_z dangling bond	mixed Al-Si	Si p_z-like long. backbond
E	Al p_z-like σ^* antibond	Si p_z-like Al *s*-like	Si p_z-like Al *s*-like	Si p_{xy}-like transv. backbond
F	...	Al p_{xy}-like	Si p_z-like Al *s*-like	Al p_z dangling bond
G	...	...	Si p_z Al s, p_z	...
H	...	...	Al p_{xy}	

IV. DISCUSSION AND COMPARISON TO EXPERIMENT

In this section we shortly review recent spectroscopic experimental data on Si(111) surfaces with metal overlayers. The main results are compared to our calculations and conclusions as to the electronic and structural nature of the metal-semiconductor interface are drawn.

Recent experiments include low-energy-electron diffraction (LEED),[16,17,21] UPS,[16] and EELS[13,17,21] measurements. All experiments are done on previously sputtered and annealed Si(111) surfaces, which at temperatures below 700 °C exhibit the well known *intrinsic* 7×7 LEED pattern. The metal deposition is usually done around 100–200 °C and the *intrinsic* 7×7 pattern is changed into a sharp *extrinsic* 7×7 pattern for submonolayer metal coverages. For higher coverages ($\Theta > 0.5$) the $\frac{1}{7}$ order spots begin to disappear. Subsequent annealing of the metal-covered surface diffuses the extrinsic 7×7 pattern drastically. The deposition of metal onto hot surfaces has also been studied and yields yet another variation of the 7×7 LEED pattern.[21,24] In fact the original Lander substitutional model has been proposed for metal chemisorption on hot ($T > 500$ °C) surfaces.[24] Considerably more experimental studies, however, have been done for cold surfaces and we thus shall concentrate on them.

The low-temperature LEED results suggest that

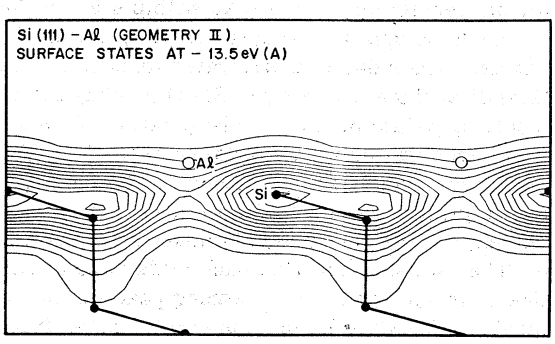

FIG. 8. Charge-density-contour plot for the Si *s*-like surface states around −13.5 eV in geometry II (peak A). The contours are given in a (110) plane perpendicular to the (111) surface and are arbitrarily normalized.

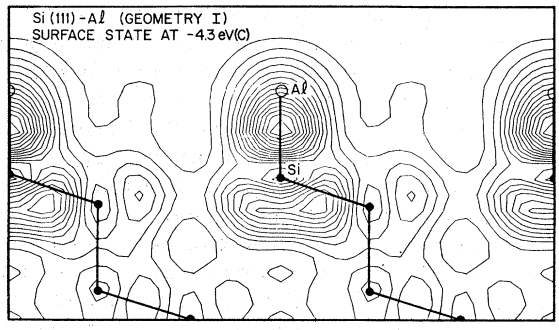

FIG. 9. Charge-density-contour plot for the surface state around −4.3 eV in geometry I (peak *C*).

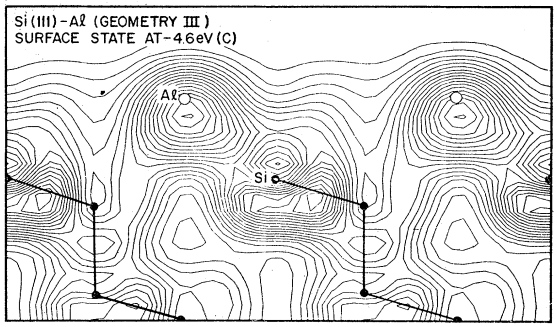

FIG. 10. Charge-density-contour plot for the surface state around −4.6 eV in geometry III (peak *C*).

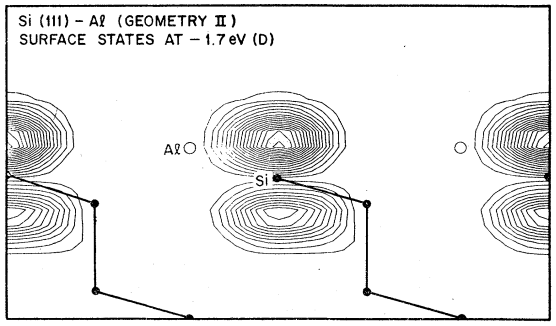

FIG. 12. Charge-density-contour plot for the surface state around −1.7 eV in geometry II (peak *D*).

for submonolayer coverage the metal atoms chemisorb in well-defined sites on the Si(111) 7× 7 surface. With higher degrees of coverage aggregation of aluminum may occur. Additional evidence for this aggregation is given by the observation of strong aluminum bulk and surface plasmon losses in EEL spectroscopy for coverages of about two monolayers.[21] Thin uniform layers of this thickness are not expected to exhibit the well-defined loss peaks.

While the Si(111) 7× 7 surface is the thermodynamically stable surface and easily experimentally obtained, no clear unambiguous theoretical model exists for this reconstructed surface. The available theoretical results are all obtained for an ideal, unreconstructed 1× 1 surface or for the 2× 1 reconstruction and therefore caution has to be used in comparing theory and experiment. Since the Si(111) 2× 1 reconstruction which occurs upon cleavage is believed to be only a small perturbation on the ideal unreconstructed surface it would, from the theoretical point of view, be desirable to repeat the spectroscopic experiments on freshly cleaved Si(111) surfaces. Nonetheless, comparisons of the present experimental and theoretical results can still be meaningful if they are guided by reasonable models of the 7× 7 reconstruction. One such model, containing a high percentage of lattice vacancies in the outermost Si layer has originally been proposed by Lander[24] and since been regarded on the basis of various experiments, as the *most probable* of all models. We shall therefore try to accommodate the essential features of the vacancy model in the following discussion.

The UPS spectra reported in Ref. 16 indicate relative shifts of Fermi level and vacuum level with respect to the Si band structure when metals are deposited. In Fig. 14 we show a typical variation of these energies with metal overlayer thickness as obtained experimentally in Ref. 16. We note that most remarkably for an overlayer thickness of about 2 Å (i.e., about 1–2 monolayers) the Fermi level is fully stabilized and thus the Schottky barrier height is determined. Based on this important observation the present studies are of significance for Schottky barrier formation. It is further observed that the Fermi level drops from 0.55 eV (above E_v) for the clean 7× 7 surface to 0.35 eV for the Al covered surface. As pointed out in Sec. III we find a significant drop of E_F in the calculations only if Al is chemisorbed on Si(111) in the "covalent" on-top position (case I). However, we shall not use this observation as

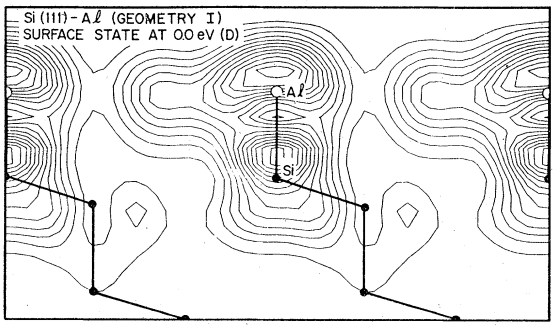

FIG. 11. Charge-density-contour plot for the surface state around 0.0 eV in geometry I (peak *D*).

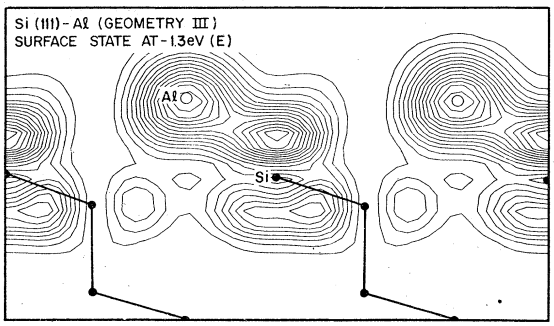

FIG. 13. Charge-density-contour plot for the surface state around −1.3 eV in geometry III (peak *E*).

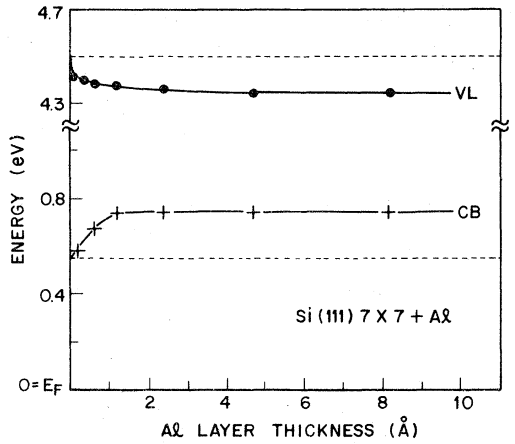

FIG. 14. Experimental results of Ref. 16 describing the position of the conduction band minimum (CB) and the vacuum level (VI) vs Al coverage of Si(111) 7×7. The dashed lines correspond to the clean surface position. The energies are referred to the Fermi level.

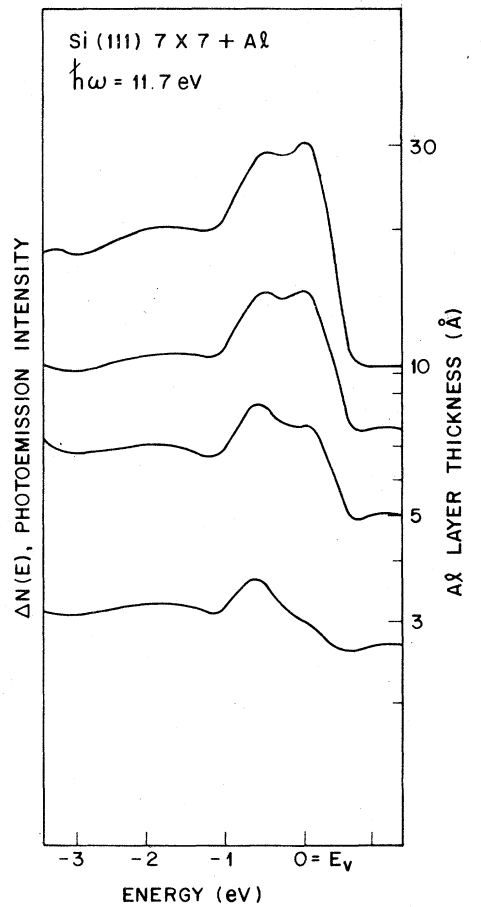

FIG. 15. Experimental results of Ref. 16 showing UPS difference between clean and Al-covered Si(111). The energies are referred to the top of the silicon bulk valence bands.

strong support for the occurrence of the onefold covalent site for Al chemisorption, since reconstruction effects may be of importance in this regard but are completely left out of consideration.

As also seen from Fig. 14 the vacuum level drops even more drastically from 5.05 ± 0.1 eV for clean 7×7 silicon (111) to 4.70 ± 0.1 eV for metal-covered silicon (111). This drop is rather independent of the kind of metal (i.e., Al, Ga, In) deposited and has qualitatively also been found in our calculations and in the work of Ref. 23. The drop in the work function or electron affinity is in accord with the simple rule that less-electronegative chemisorbed species should lower the surface dipole and thus the work function. In the present case this rule has to be refined somewhat due to the presence of pronounced dangling bond charges on clean Si(111). This effect has been found to be of importance for hydrogen chemisorption on Si(111).[31]

To study the effect of metal coverage via UPS one conveniently takes the difference between spectra obtained on clean and on metal-covered surfaces. For this purpose the spectra have to be aligned at some *bulk* silicon feature to remove spurious derivative effects due to changes in band bending. Experimental difference spectra of Ref. 16 are shown in Fig. 15. It is evident from these curves that the metal coverage causes a decrease of the density of states above E_V near E_F. It has been shown[32] that the states which are removed are strongly localized near the surface, and that their origin is related to the silicon dangling-bond and back-bond states. In addition several metal-related features occur in the spectra around 0.0, −0.55, and −1.95 eV. These peaks do *not* correspond to features in the pure metal photoemission spectra[16] but are related to chemical bonds formed at the interface. In combination with EELS data, reported in Refs. 17 and 21 these structures may be used to discriminate on the basis of our calculations between the various structural models. The important energies are listed in Table IV. From the comparison between theory and experiment (see Figs. 7 and 14 and Table IV) it follows that the "covalent" on-top geometry (case I) is unlikely to occur for Al chemisorption on Si(111). Some intermediate case between II and III which corresponds to the "ionic" threefold chemisorption site with some intermediate bond length seems to yield the best agreement along with the results of the Lander substitutional geometry.

On the basis of the UPS data one may thus propose that Al chemisorbs on Si(111) in threefold coordinated "ionic" sites and if vacancies are present in the 7×7 reconstruction, additional Al may fill these vacancies in accord with the Lander substitutional model. It should be noted that no

TABLE IV. Comparison of experimental spectroscopic energies and calculated peak positions for the four different geometries. All energies are measured with respect to the Si valence-band maximum. The labeling of the calculated peaks corresponds to Fig. 7.

	Experiment				Theory			
					Geometry			
	UPS Ref. 16	core[a] EELS Ref. 13	EELS Ref. 17	EELS Ref. 21	I	II	III	Lander Ref. 23
Energies	-1.95				...	-1.7*D*	-2.5*D*	-1.6*D*
	-0.55				...	...	-1.3*E*	...
	~0.0				0.0*D*	0.2*E*	0.7*F*	0.1*E*
		0.5-1.1			...	2.0*F*	1.5*G*	1.5*F*
Energy Differences				1.9				1.6*E-F*
			2.8	3.2			2.8*E-G*	3.1*D-F*
			4.0	4.9		3.7*D-F*	4.0*D-G*	
				7.1				

[a] Si(111) with Ga overlayers. Excitation from Ga-3*d* core.

strong structure is found in the experimental UPS spectra around −4.6 eV, whereas *all* theoretical calculations yield a strong peak in this energy region corresponding to Al *s* levels. The discrepancy is probably due to matrix element effects which are known to suppress *s*-like initial states in UPS experiments.

The main results obtained with EELS are the removal of clean-surface spectral features at an early stage of metal coverage while the bulk silicon features remain almost unchanged, and the appearance of new metal-related peaks. In particular the surface excitations commonly labelled S_1, S_2, and S_3 disappear while two prominent new structures are reported to appear at 2.8 and 4.0 eV.[17] As far as the energies of the new peaks are concerned there are some discrepancies between the results of Refs. 17 and 21 (see Table IV). The two new losses at 2.8 and 4.0 eV can be explained as transition between valence band features and the same final-state feature, i.e., a strongly resonant state within the silicon gap. Evidence for the existence of this final state is also reported from core level EELS on the Si(111)-Ga system.[13] The assumption of such a final-state structure again favors the threefold ionic sites and the Lander substitutional geometry over the onefold covalent site.

V. CONCLUSIONS

The most important points emerging from a comparison of the present theoretical studies with recent UPS and EELS studies on Schottky barrier formation on Si(111) are as follows:

(i) Fermi-level pinning occurs with monolayer metal coverage due to the formation of metal-semiconductor covalent bonding and banding effects. Thus, studies of monolayer metal chemisorption on Si(111) are relevant for the understanding of Schottky barrier formation.

(ii) Individual surface-state features observed on clean Si(111) are changed or removed and replaced by specific metal-induced interface state features. In particular within several eV of the Fermi level prominent structures are found in both experiment and theoretical calculations which take into account the discrete lattice structure. No such features are found in earlier silicon-jellium calculations.[7]

(iii) A detailed analysis of spectral energies shows the appearance of an empty final-state feature within the silicon gap and at least three occupied initial-state features within 4 eV of the valence band edge. The existence and energetic positions of these structures support the threefold ionic geometry along with the Lander substitutional geometry for Al chemisorption on Si(111) 7×7.

ACKNOWLEDGMENTS

The authors thank Dr. J. E. Rowe, Dr. G. Margaritondo, and Dr. J. R. Chelikowsky for helpful discussions. We also thank K. M. Ho for providing us with the exchange potential programs using FFT routines.

*Present address, Dept. of Physics, Seoul National University, Seoul, Korea.
[1]For a review see S. M. Sze, *Physics of Semiconductor Devices* (Wiley, New York, 1969); A. G. Milnes and D. L. Feucht, *Heterojunctions and Metal-Semiconductor Junctions* (Academic, New York, 1972).
[2]S. Kurtin, T. C. McGill, and C. A. Mead, Phys. Rev. Lett. 22, 1433 (1969).
[3]J. C. Phillips, *Bonds and Bands in Semiconductors* (Academic, New York, 1973).
[4]J. C. Inkson, J. Phys. C 5, 2599 (1972); 6, 1350 (1973); J. Vac. Sci. Technol. 11, 943 (1974).
[5]J. C. Phillips, J. Vac. Sci. Technol. 11, 947 (1974).
[6]E. Louis, F. Yndurain, and F. Flores, Phys. Rev. B 13, 4408 (1976); C. Tejedor, F. Flores, and E. Louis, J. Phys. C 10, 2163 (1977).
[7]S. G. Louie and Marvin L. Cohen, Phys. Rev. Lett. 35, 866 (1975); Phys. Rev. B 13, 2461 (1975); S. G. Louie, J. R. Chelikowsky, and Marvin L. Cohen, J. Vac. Sci. Technol. 13, 790 (1976).
[8]E. J. Mele and J. D. Joannopoulos (unpublished).
[9]C. M. Varma and K. C. Pandey (unpublished).
[10]M. Schlüter (unpublished).
[11]J. Bardeen, Phys. Rev. 71, 717 (1947).
[12]V. Heine, Phys. Rev. 138, A1689 (1965).
[13]J. E. Rowe, S. B. Christman, and G. Margaritondo, Phys. Rev. Lett. 35, 1471 (1975).
[14]G. Margaritondo, S. B. Christman, and J. E. Rowe, J. Vac. Sci. Technol. 13, 329 (1976).
[15]J. E. Rowe, J. Vac. Sci. Techol. 13, 798 (1976).
[16]G. Margaritondo, J. E. Rowe, and S. B. Christman, Phys. Rev. B 14, 5396 (1976).
[17]J. E. Rowe, G. Margaritondo, and S. B. Christman, Phys. Rev. B 15, 2195 (1977).
[18]D. E. Eastman and J. L. Freeouf, Phys. Rev. Lett. 34, 1624 (1975).
[19]P. W. Chye, I. A. Babalola, T. Sukegawa, and W. E. Spicer, Phys. Rev. Lett. 35, 1602 (1975); W. E. Spicer, P. E. Gregory, P. W. Chye, I. A. Babalola, and T. Sukegawa, Appl. Phys. Lett. 27, 617 (1975); P. E. Gregory and W. E. Spicer, Phys. Rev. B 12, 2370 (1975).
[20]L. J. Brillson, Phys. Rev. Lett. 38, 245 (1977) and (unpublished).
[21]Y. W Chung, W. Siekhaus, and G. Somorjai, Phys. Rev. B 15, 959 (1977).
[22]J. A. Appelbaum and D. R. Hamann, *Proceedings of the 12th International Conference on the Physics of Semiconductors* (Teubner, Stuttgart, 1974), p. 675.
[23]J. R. Chelikowsky, Phys. Rev. B 16, 3618 (1977).
[24]J. J. Lander and J. Morrison, Surf. Sci. 2, 553 (1964).
[25]M. Schlüter, J. R. Chelikowsky, S. G. Louie, and Marvin L. Cohen, Phys. Rev. B 12, 4200 (1975).
[26]M. Schlüter, J. E. Rowe, G. Margaritondo, K. M. Ho, and Marvin L. Cohen, Phys. Rev. Lett. 37, 1632 (1976); K. M. Ho, M. Schlüter, and Marvin L. Cohen (unpublished).
[27]F. Herman and S. Skillman, *Atomic Structure Calculations* (Prentice Hall, Englewood Cliffs, N. J., 1963).
[28]K. M. Ho (private communication).
[29]A. Baldereschi, Phys. Rev. B 7, 5212 (1973); D. J. Chadi and Marvin L. Cohen, Phys. Rev. B 8, 5747 (1973).
[30]G. Gilat and L. J. Raubenheimer, Phys. Rev. 144, 390 (1966).
[31]J. A. Appelbaum and D. R. Hamann, Phys. Rev. Lett. 34, 806 (1975).
[32]L. F. Wagner and W. E. Spicer, Phys. Rev. Lett. 28, 1381 (1972); D. E. Eastman and W. D. Grobman, *ibid.* 28, 1378 (1972); J. E. Rowe and H. Ibach, *ibid.* 32, 421 (1974).